Thermal stresses and deflections of functionally graded sandwich plates using a new refined hyperbolic shear deformation theory

Ali Bouchafa [1], Mohamed Bachir Bouiadjra [2],
Mohammed Sid Ahmed Houari [2,3] and Abdelouahed Tounsi [*1,2]

[1] *Material and Hydrology Laboratory, University of Sidi Bel Abbes,
Faculty of Technology, Civil Engineering Department, Algeria*
[2] *Laboratoire des Structures et Matériaux Avancés dans le Génie Civil et Travaux Publics,
Université de Sidi Bel Abbes, Faculté de Technologie, Département de génie civil, Algeria*
[2] *Département de génie civil, Université de Mascara, Algeria*

Abstract. A new refined hyperbolic shear deformation theory (RHSDT), which involves only four unknown functions as against five in case of other shear deformation theories, is presented for the thermoelastic bending analysis of functionally graded sandwich plates. Unlike any other theory, the number of unknown functions involved is only four, as against five in case of other shear deformation theories. The theory presented is variationally consistent, does not require shear correction factor, and gives rise to transverse shear stress variation such that the transverse shear stresses vary parabolically across the thickness satisfying shear stress free surface conditions. The sandwich plate faces are assumed to have isotropic, two-constituent material distribution through the thickness, and the modulus of elasticity, Poisson's ratio of the faces, and thermal expansion coefficients are assumed to vary according to a power law distribution in terms of the volume fractions of the constituents. The core layer is still homogeneous and made of an isotropic ceramic material. Several kinds of sandwich plates are used taking into account the symmetry of the plate and the thickness of each layer. The influences played by the transverse shear deformation, thermal load, plate aspect ratio and volume fraction distribution are studied. Numerical results for deflections and stresses of functionally graded metal–ceramic plates are investigated. It can be concluded that the proposed theory is accurate and simple in solving the thermoelastic bending behavior of functionally graded plates.

Keywords: hyperbolic plate theory; thermoelastic bending response; functionally graded material; sandwich plate

1. Introduction

Functionally graded materials (FGMs) are special composites whose material properties vary continuously through their thickness. FGMs are usually made of mixture of ceramic and metal, and can thus resist high-temperature environments while maintaining toughness. The technology

---

∗Corresponding author, Professor, E-mail: tou_abdel@yahoo.com

of FGMs was an original material fabrication technology proposed in Japan in 1984 by Sendai Group. FGMs are used in very different applications, such as reactor vessels, fusion energy devices, biomedical sectors, aircrafts, space vehicles, defense industries and other engineering structures. Indeed, the mechanical behavior of structural members with FGMs is of considerable importance in both research and industrial fields (Lu *et al*. 2009, Talha and Singh 2010, Wen *et al*. 2011, Jha *et al*. 2013, Bessaim *et al*. 2013, Chakraverty and Pradhan 2014, Bousahla *et al*. 2014, Ait Yahia *et al*. 2015, Bourada *et al*. 2015).

The advantage of using FGMs is that they able to withstand high temperature gradient environments while maintaining their structural integrity. For example, in a conventional thermal barrier coating for high-temperature applications, a discrete layer of ceramic material is bounded to a metallic structure. However, the abrupt transition in material properties across the interface between distinct materials can cause large interlaminar stresses and leads to plastic deformation or cracking (Finot and Suresh 1996). These adverse effects can be alleviated by functionally grading the material to have a smooth spatial variation of material composition, with ceramic-rich material placed at the high-temperature locations and metal-rich material in regions where mechanical properties need to be high.

In recent years, studies on FGM structures in thermal environments are an altercative emerging area in the research community. Obata and Noda (1994) have investigated 1D steady-state thermal stresses in a FG hollow sphere and a FG hollow circular cylinder using a perturbation approach. Reddy and Chin (1998) have developed coupled as well as uncoupled thermoelastic finite element formulation for analyzing the thermomechanical behavior of FG cylinders and plates subjected to abrupt thermal loading. Praveen *et al*. (1999) have developed a thermoelastic finite element model to study the response of a FG cylinder subjected to rapid heating. The analysis takes into account the material properties variations with temperature. Vel and Barta (2002, 2003) have presented exact 3D solutions for the steady-state and quasi static transient thermoelastic response of a thick plate with an arbitrary variation of material properties in the thickness direction. Ying *et al*. (2009) investigated thermal deformations of FGM thick plates using a semi-analytical method. A novel refined hyperbolic shear deformation theory was developed by El Meiche *et al*. (2011) utilizing Navier's solution technique for buckling and free vibration analysis of FG sandwich plates. Ould Larbi *et al*. (2013) presented an efficient shear deformation beam theory based on neutral surface position for bending and free vibration of FG beams. Recently, the post-buckling and nonlinear free vibration behaviors of geometrically imperfect FG beams supported by nonlinear elastic foundation are studied by Yaghoobi and Torabi (2013a). Yaghoobi and Torabi (2013b) presented exact solution for thermal buckling of FG plates resting on elastic foundations with various boundary conditions. An analytical approach is developed by Yaghoobi and Yaghoobi (2013) for buckling analysis of sandwich plates with FGM face sheets resting on elastic foundation with various boundary conditions. Belabed *et al*. (2014) proposed an efficient and simple higher order shear and normal deformation theory for FG plates. Hebali *et al*. (2014) developed a new quasi-three-dimensional (3D) hyperbolic shear deformation theory for the bending and free vibration analysis of FG plate. Fekrar *et al*. (2014) developed a new five-unknown refined theory based on neutral surface position for bending analysis of exponential graded plates. In the same way, Hamidi *et al*. (2015) proposed a sinusoidal plate theory with 5-unknowns and stretching effect for thermo-mechanical bending analysis of FG sandwich plates. Houari *et al*. (2013) analyzed the sandwich plates with functionally graded skins under thermal load by using a higher order shear deformation theory with thickness stretching effect. Attia *et al*. (2015) studied the free vibration response of FG plates with temperature-dependent properties using various four variable

refined plate theories. Mahi *et al*. (2015) developed a new hyperbolic shear deformation theory for bending and free vibration analysis of isotropic, functionally graded, sandwich and laminated composite plates with various boundary conditions. Swaminathan and Naveenkumar (2014) presented higher order refined computational models for the stability analysis of FG plates. Mantari and Granados (2015) presented a new quasi-3D hybrid type higher order shear deformation theory for thermoelastic bending analysis of functionally graded sandwich plates.

The objective of this investigation is to develop a simple and efficient theory for thermoelastic bending of FGM sandwich plates. Various higher-order shear deformation theories involve use of five unknown functions. The well-known higher-order plate theories are as follows: (i) parabolic shear deformation plate theory (PSDPT) Reddy (1984); (ii) sinusoidal shear deformation plate theory (SSDPT) Touratier (1991); and (iii) exponential shear deformation plate theory (ESDPT) Karama *et al*. (2003). Recently, four variable refined plate theories (Draiche *et al*. 2014, Ait Amar Meziane *et al*. 2014, Yaghoobi and Fereidoon 2014, Nedri *et al*. 2014, Zidi *et al*. 2014, Khalfi *et al*. 2013, Bouderba *et al*. 2013, Bachir Bouiadjra *et al*. 2013, Tounsi *et al*. 2013, Bourada *et al*. 2012, Benachour *et al*. 2011) are developed for FGM plates.

In this paper a new refined hyperbolic shear deformable plate theory (RHSDT) is used for thermoelastic bending of FGM sandwich plates. The hyperbolic function in terms of thickness coordinate is used in the displacement field to account for shear deformation. The novel feature of the theory is that it does not require shear correction factor and satisfying the shear-stress-free boundary conditions at top and bottom of the plate. The effects of temperature field on the dimensionless axial and transverse shear stresses and deflection of the FGM sandwich plate are studied. Numerical examples are presented to illustrate the accuracy and efficiency of the present theory by comparing the obtained results with those computed using various other theories.

2. Problem formulation

Consider the case of a uniform thickness, rectangular FGM sandwich plate composed of three microscopically heterogeneous layers referring to rectangular coordinates (x, y, z) as shown in Fig. 1. The top and bottom faces of the plate are at $z = \pm h / 2$, and the edges of the plate are parallel to axes x and y.
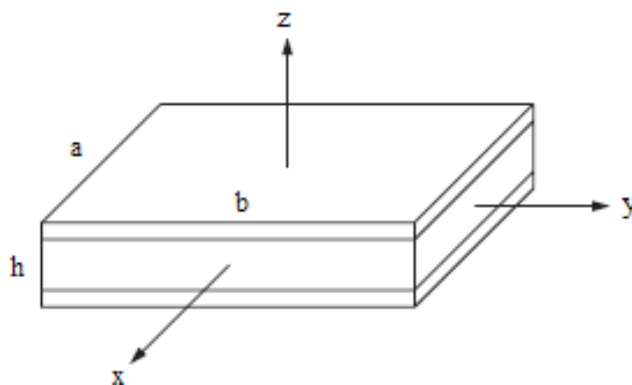

Fig. 1 Geometry of rectangular FGM sandwich plate with uniform thickness in the rectangular Cartesian coordinates
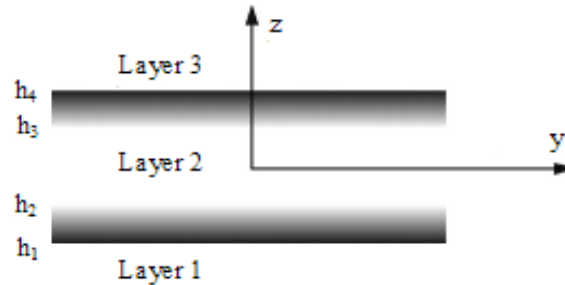
Fig. 2 The material variation along the thickness of the FGM sandwich plate

The sandwich plate is composed of three elastic layers, namely, ''Layer 1'', ''Layer 2'', and ''Layer 3'' from bottom to top of the plate (Fig. 2). The vertical ordinates of the bottom, the two interfaces, and the top are denoted by $h_1 = - h / 2$, h_2, h_3, $h_4 = h / 2$, respectively. For the brevity, the ratio of the thickness of each layer from bottom to top is denoted by the combination of three numbers, i.e., ''1-0-1'', ''2-1-2'' and so on.

The volume fraction of the FGMs is assumed to obey a power-law function along the thickness direction

$$V^{(1)} = \left(\frac{z - h_1}{h_2 - h_1}\right)^k, \qquad z \in [h_1, \ h_2] \tag{1a}$$

$$V^{(2)} = 1, \qquad z \in [h_2, \ h_3] \tag{1b}$$

$$V^{(3)} = \left(\frac{z - h_4}{h_3 - h_4}\right)^k, \qquad z \in [h_3, \ h_4] \tag{1c}$$

where $V^{(n)}$, ($n = 1, 2, 3$) denotes the volume fraction function of layer n; k is the volume fraction index ($0 \leq k \leq +\infty$), which indicates the material variation profile through the thickness.

The effective material properties, like Young's modulus E, Poisson's ratio v, and thermal expansion coefficient α then can be expressed by the rule of mixture (Marur 1999) as

$$P^{(n)}(z) = P_2 + (P_1 - P_2) V^{(n)} \tag{2}$$

where $P^{(n)}$ is the effective material property of FGM of layer n. P_2 and P_1 denote the property of the bottom and top faces of layer 1 ($h_1 \leq z \leq h_2$), respectively, and vice versa for layer 3 ($h_3 \leq z \leq h_4$) depending on the volume fraction $V^{(n)}$ ($n = 1, 2, 3$). For simplicity, Poisson's ratio of plate is assumed to be constant in this study for that the effect of Poisson's ratio on the deformation is much less than that of Young's modulus (Delale and Erdogan 1983).

2.1 Higher-order plate theory

The displacements of a material point located at (x, y, z) in the plate may be written as

$$u = u_0(x, y) - z\frac{\partial w_0}{\partial x} + \Psi(z)\,\theta_x \tag{3a}$$

$$v = v_0(x, y) - z\frac{\partial w_0}{\partial y} + \Psi(z)\,\theta_y \tag{3b}$$

$$w = w_0(x, y) \tag{3c}$$

where, u, v, w are displacements in the x, y, z directions, u_0, v_0 and w_0 are midplane displacements, θ_x and θ_y rotations of the yz and xz planes due to bending, respectively. $\Psi(z)$ represents shape function determining the distribution of the transverse shear strains and stresses along the thickness. The displacement field of the classical thin plate theory (CPT) is obtained easily by setting $\Psi(z) = 0$. The displacement of the first-order shear deformation plate theory (FSDPT) is obtained by setting $\Psi(z) = z$. Also, the displacement of parabolic shear deformation plate theory (PSDPT) of Reddy (1984) is obtained by setting

$$\Psi(z) = z\left(1 - \frac{4z^2}{3h^2}\right) \tag{4a}$$

The sinusoidal shear deformation plate theory (SSDPT) of Touratier (1991) is obtained by setting

$$\Psi(z) = \frac{h}{\pi}\sin\left(\frac{\pi z}{h}\right) \tag{4b}$$

In addition, the exponential shear deformation plate theory (ESDPT) of Karama *et al.* (2003) is obtained by setting

$$\Psi(z) = ze^{-2(z/h)^2} \tag{4c}$$

2.2 Present refined hyperbolic shear deformation theory

Unlike the other theories, the number of unknown functions involved in the present refined hyperbolic shear deformation theory (RHSDT) is only four, as against five in case of other shear deformation theories (Reddy 1984, Touratier 1991, Karama *et al.* 2003). The theory presented is variationally consistent, does not require shear correction factor, and gives rise to transverse shear stress variation such that the transverse shear stresses vary parabolically across the thickness satisfying shear stress free surface conditions.

2.2.1 Assumptions of the present plate theory (RHSDT)
Assumptions of the (RHSDT) are as follows:

(1) The displacements are small in comparison with the plate thickness and, therefore, strains involved are infinitesimal.
(2) The transverse displacement w includes two components of bending w_b, and shear w_s. These components are functions of coordinates x, y only.

$$w(x, y, z) = w_b(x, y) + w_s(x, y) \tag{5}$$

(3) The transverse normal stress σ_z is negligible in comparison with in-plane stresses σ_x and σ_y.
(4) The displacements u in x-direction and v in y-direction consist of extension, bending, and shear components.

$$U = u_0 + u_b + u_s, \qquad V = v_0 + v_b + v_s \qquad (6)$$

The bending components u_b and v_b are assumed to be similar to the displacements given by the classical plate theory. Therefore, the expression for u_b and v_b can be given as

$$u_b = -z\frac{\partial w_b}{\partial x}, \qquad v_b = -z\frac{\partial w_b}{\partial y} \qquad (7)$$

The shear components u_s and v_s give rise, in conjunction with w_s, to the parabolic variations of shear strains γ_{xz}, γ_{yz} and hence to shear stresses τ_{xz}, τ_{yz} through the thickness of the plate in such a way that shear stresses τ_{xz}, τ_{yz} are zero at the top and bottom faces of the plate. Consequently, the expression for u_s and v_s can be given as

$$u_s = -f(z)\frac{\partial w_s}{\partial x}, \qquad v_s = -f(z)\frac{\partial w_s}{\partial y} \qquad (8)$$

2.2.2 Kinematics and constitutive equations

Based on the assumptions made in the preceding section, the displacement field can be obtained using Eqs. (5)-(8) as

$$u(x,y,z) = u_0(x,y) - z\frac{\partial w_b}{\partial x} - f(z)\frac{\partial w_s}{\partial x}$$

$$v(x,y,z) = v_0(x,y) - z\frac{\partial w_b}{\partial y} - f(z)\frac{\partial w_s}{\partial y} \qquad (9a)$$

$$w(x,y,z) = w_b(x,y) + w_s(x,y)$$

where

$$f(z) = \frac{(h/\pi)\sinh\left(\dfrac{\pi}{h}z\right) - z}{[\cosh(\pi/2) - 1]} \qquad (9b)$$

The strains associated with the displacements in Eq. (9) are

$$\varepsilon_x = \varepsilon_x^0 + z\,k_x^b + f(z)\,k_x^s$$

$$\varepsilon_y = \varepsilon_y^0 + z\,k_y^b + f(z)\,k_y^s$$

$$\gamma_{xy} = \gamma_{xy}^0 + z\,k_{xy}^b + f(z)\,k_{xy}^s \qquad (10)$$

$$\gamma_{yz} = g(z)\,\gamma_{yz}^s$$

$$\gamma_{xz} = g(z)\,\gamma_{xz}^s$$

$$\varepsilon_z = 0$$

where

$$\varepsilon_x^0 = \frac{\partial u_0}{\partial x}, \qquad k_x^b = -\frac{\partial^2 w_b}{\partial x^2}, \qquad k_x^s = -\frac{\partial^2 w_s}{\partial x^2},$$

$$\varepsilon_y^0 = \frac{\partial v_0}{\partial y}, \qquad k_y^b = -\frac{\partial^2 w_b}{\partial y^2}, \qquad k_y^s = -\frac{\partial^2 w_s}{\partial y^2}$$

$$\gamma_{xy}^0 = \frac{\partial u_0}{\partial y} + \frac{\partial v_0}{\partial x}, \quad k_{xy}^b = -2\frac{\partial^2 w_b}{\partial x \partial y}, \quad k_{xy}^s = -2\frac{\partial^2 w_s}{\partial x \partial y}$$

$$\gamma_{xz}^s = \frac{\partial w_s}{\partial x}, \qquad g(z) = 1 - f'(z) \quad \text{and} \quad f'(z) = \frac{df(z)}{dz}$$

(11)

For elastic and isotropic FGMs, the constitutive relations can be written as:

$$\begin{Bmatrix} \sigma_x \\ \sigma_y \\ \tau_{xy} \end{Bmatrix}^{(n)} = \begin{bmatrix} Q_{11} & Q_{12} & 0 \\ Q_{12} & Q_{22} & 0 \\ 0 & 0 & Q_{66} \end{bmatrix}^{(n)} \begin{Bmatrix} \varepsilon_x - \alpha T \\ \varepsilon_y - \alpha T \\ \gamma_{xy} \end{Bmatrix}^{(n)} \quad \text{and} \quad \begin{Bmatrix} \tau_{yz} \\ \tau_{zx} \end{Bmatrix}^{(n)} = \begin{bmatrix} Q_{44} & 0 \\ 0 & Q_{55} \end{bmatrix}^{(n)} \begin{Bmatrix} \gamma_{yz} \\ \gamma_{zx} \end{Bmatrix}^{(n)}$$

(12)

where $(\sigma_x, \sigma_y, \tau_{xz}, \tau_{yz}, \tau_{yx})$ and $(\varepsilon_x, \varepsilon_y, \gamma_{xy}, \gamma_{yz}, \gamma_{yx})$ are the stress and strain components, respectively. Using the material properties defined in Eq. (2), stiffness coefficients, Q_{ij}, can be expressed as

$$Q_{11} = Q_{22} = \frac{E(z)}{1 - v^2},$$

(13a)

$$Q_{12} = \frac{v\,E(z)}{1 - v^2},$$

(13b)

$$Q_{44} = Q_{55} = Q_{66} = \frac{E(z)}{2(1 + v)},$$

(13c)

2.3 Governing equations

The governing equations of equilibrium can be derived by using the principle of virtual displacements. The principle of virtual work in the present case yields

$$\int_{-h/2}^{h/2} \int_{\Omega} \left[\sigma_x \delta \varepsilon_x + \sigma_y \delta \varepsilon_y + \tau_{xy} \delta \gamma_{xy} + \tau_{yz} \delta \gamma_{yz} + \tau_{xz} \delta \gamma_{xz} \right] d\Omega \, dz = 0$$

(14)

where Ω is the top surface.

Substituting Eqs. (10) and (12) into Eq. (14) and integrating through the thickness of the plate, Eq. (14) can be rewritten as

$$\int_{\Omega} \left[N_x \delta \varepsilon_x^0 + N_y \delta \varepsilon_y^0 + N_{xy} \delta \varepsilon_{xy}^0 + M_x^b \delta k_x^b + M_y^b \delta k_y^b + M_{xy}^b \delta k_{xy}^b + M_x^s \delta k_x^s \right.$$
$$\left. + M_y^s \delta k_y^s + M_{xy}^s \delta k_{xy}^s + S_{yz}^s \delta \gamma_{yz}^s + S_{xz}^s \delta \gamma_{xz}^s \right] d\Omega = 0$$

(15)

where

$$\begin{Bmatrix} N_x, & N_y, & N_{xy} \\ M_x^b, & M_y^b, & M_{xy}^b \\ M_x^s, & M_y^s, & M_{xy}^s \end{Bmatrix} = \sum_{n=1}^{3} \int_{h_n}^{h_{n+1}} (\sigma_x, \sigma_y, \tau_{xy})^{(n)} \begin{Bmatrix} 1 \\ z \\ f(z) \end{Bmatrix} dz, \qquad (16a)$$

$$(S_{xz}^s, S_{yz}^s) = \sum_{n=1}^{3} \int_{h_n}^{h_{n+1}} (\tau_{xz}, \tau_{yz})^{(n)} g(z) dz. \qquad (16b)$$

where h_{n+1} and h_n are the top and bottom z-coordinates of the nth layer.

The governing equations of equilibrium can be derived from Eq. (15) by integrating the displacement gradients by parts and setting the coefficients δu_0, δv_0, δw_b and δw_s zero separately. Thus one can obtain the equilibrium equations associated with the present shear deformation theory

$$\delta u: \quad \frac{\partial N_x}{\partial x} + \frac{\partial N_{xy}}{\partial y} = 0$$

$$\delta v: \quad \frac{\partial N_{xy}}{\partial x} + \frac{\partial N_y}{\partial y} = 0$$

$$\delta w_b: \quad \frac{\partial^2 M_x^b}{\partial x^2} + 2\frac{\partial^2 M_{xy}^b}{\partial x \partial y} + \frac{\partial^2 M_y^b}{\partial y^2} = 0 \qquad (17)$$

$$\delta w_s: \quad \frac{\partial^2 M_x^s}{\partial x^2} + 2\frac{\partial^2 M_{xy}^s}{\partial x \partial y} + \frac{\partial^2 M_y^s}{\partial y^2} + \frac{\partial S_{xz}^s}{\partial x} + \frac{\partial S_{yz}^s}{\partial y} = 0$$

Using Eq. (12) in Eq. (16), the stress resultants of a sandwich plate made up of three layers can be related to the total strains by

$$\begin{Bmatrix} N \\ M^b \\ M^s \end{Bmatrix} = \begin{bmatrix} A & B & B^s \\ B & D & D^s \\ B^s & D^s & H^s \end{bmatrix} \begin{Bmatrix} \varepsilon \\ k^b \\ k^s \end{Bmatrix} - \begin{Bmatrix} N^T \\ M^{bT} \\ M^{sT} \end{Bmatrix}, \qquad S = A^s \gamma, \qquad (18)$$

where

$$N = \{N_x, N_y, N_{xy}\}^t, \quad M^b = \{M_x^b, M_y^b, M_{xy}^b\}^t, \quad M^s = \{M_x^s, M_y^s, M_{xy}^s\}^t, \qquad (19a)$$

$$N^T = \{N_x^T, N_y^T, 0\}^t, \quad M^{bT} = \{M_x^{bT}, M_y^{bT}, 0\}^t, \quad M^{sT} = \{M_x^{sT}, M_y^{sT}, 0\}^t, \qquad (19b)$$

$$\varepsilon = \{\varepsilon_x^0, \varepsilon_y^0, \gamma_{xy}^0\}^t, \quad k^b = \{k_x^b, k_y^b, k_{xy}^b\}^t, \quad k^s = \{k_x^s, k_y^s, k_{xy}^s\}^t, \qquad (19c)$$

$$A = \begin{bmatrix} A_{11} & A_{12} & 0 \\ A_{12} & A_{22} & 0 \\ 0 & 0 & A_{66} \end{bmatrix}, \quad B = \begin{bmatrix} B_{11} & B_{12} & 0 \\ B_{12} & B_{22} & 0 \\ 0 & 0 & B_{66} \end{bmatrix}, \quad D = \begin{bmatrix} D_{11} & D_{12} & 0 \\ D_{12} & D_{22} & 0 \\ 0 & 0 & D_{66} \end{bmatrix}, \qquad (19d)$$

$$B^s = \begin{bmatrix} B_{11}^s & B_{12}^s & 0 \\ B_{12}^s & B_{22}^s & 0 \\ 0 & 0 & B_{66}^s \end{bmatrix}, \quad D^s = \begin{bmatrix} D_{11}^s & D_{12}^s & 0 \\ D_{12}^s & D_{22}^s & 0 \\ 0 & 0 & D_{66}^s \end{bmatrix}, \quad H^s = \begin{bmatrix} H_{11}^s & H_{12}^s & 0 \\ H_{12}^s & H_{22}^s & 0 \\ 0 & 0 & H_{66}^s \end{bmatrix}, \quad (19e)$$

$$S = \left\{ S_{xz}^s, S_{yz}^s \right\}^t, \quad \gamma = \left\{ \gamma_{xz}, \gamma_{yz} \right\}^t, \quad A^s = \begin{bmatrix} A_{44}^s & 0 \\ 0 & A_{55}^s \end{bmatrix}, \quad (19f)$$

where A_{ij}, B_{ij}, etc., are the plate stiffness, defined by

$$\begin{Bmatrix} A_{11} & B_{11} & D_{11} & B_{11}^s & D_{11}^s & H_{11}^s \\ A_{12} & B_{12} & D_{12} & B_{12}^s & D_{12}^s & H_{12}^s \\ A_{66} & B_{66} & D_{66} & B_{66}^s & D_{66}^s & H_{66}^s \end{Bmatrix} = \sum_{n=1}^{3} \int_{h_n}^{h_{n+1}} Q_{11}^{(n)} \left(1, z, z^2, f(z), z\, f(z), f^2(z) \right) \begin{Bmatrix} 1 \\ v^{(n)} \\ \dfrac{1-v^{(n)}}{2} \end{Bmatrix} dz \quad (20a)$$

and

$$\left(A_{22}, B_{22}, D_{22}, B_{22}^s, D_{22}^s, H_{22}^s \right) = \left(A_{11}, B_{11}, D_{11}, B_{11}^s, D_{11}^s, H_{11}^s \right), \qquad Q_{11}^{(n)} = \frac{E(z)}{1 - v^2}, \quad (20b)$$

$$A_{44}^s = A_{55}^s = \sum_{n=1}^{3} \int_{h_n}^{h_{n+1}} \frac{E(z)}{2(1+v)} \left[g(z) \right]^2 dz, \quad (20c)$$

The stress and moment resultants, $N_x^T = N_y^T$, $M_x^{bT} = M_y^{bT}$, and $M_x^{sT} = M_y^{sT}$ due to thermal loading are defined by

$$\begin{Bmatrix} N_x^T \\ M_x^{bT} \\ M_x^{sT} \end{Bmatrix} = \sum_{n=1}^{3} \int_{h_n}^{h_{n+1}} \frac{E(z)}{1-v} \alpha(z) T \begin{Bmatrix} 1 \\ z \\ f(z) \end{Bmatrix} dz, \quad (21)$$

The temperature field variation through the thickness is assumed to be

$$T(x, y, z) = T_1(x, y) + \frac{z}{h} T_2(x, y) + \frac{\Psi(z)}{h} T_3(x, y), \quad (22)$$

where T_1, T_2 and T_3 are thermal loads. In the case of the present theory (NTSDT), $\Psi(z) =$

$\dfrac{\cosh(\pi/2)}{[\cosh(\pi/2)-1]} z - \dfrac{(h/\pi)\sinh\left(\dfrac{\pi}{h} z\right)}{[\cosh(\pi/2)-1]}.$

Substituting from Eq. (18) into Eq. (17), we obtain the following equation,

$$A_{11}d_{11}u_0 + A_{66}d_{22}u_0 + (A_{12} + A_{66})d_{12}v_0 - B_{11}d_{111}w_b - (B_{12} + 2B_{66})d_{122}w_b$$
$$- (B_{12}^s + 2B_{66}^s)d_{122}w_s - B_{11}^s d_{111}w_s = p_1, \quad (23a)$$

$$A_{22}d_{22}v_0 + A_{66}d_{11}v_0 + (A_{12} + A_{66})d_{12}u_0 - B_{22}d_{222}w_b - (B_{12} + 2B_{66})d_{112}w_b$$
$$-(B_{12}^s + 2B_{66}^s)d_{112}w_s - B_{22}^s d_{222}w_s = p_2, \tag{23b}$$

$$B_{11}d_{111}u_0 + (B_{12} + 2B_{66})d_{122}u_0 + (B_{12} + 2B_{66})d_{112}v_0 + B_{22}d_{222}v_0$$
$$- D_{11}d_{1111}w_b - 2(D_{12} + 2D_{66})d_{1122}w_b$$
$$- D_{22}d_{2222}w_b - D_{11}^s d_{1111}w_s - 2(D_{12}^s + 2D_{66}^s)d_{1122}w_s - D_{22}^s d_{2222}w_s = p_3 \tag{23c}$$

$$B_{11}^s d_{111}u_0 + (B_{12}^s + 2B_{66}^s)d_{122}u_0 + (B_{12}^s + 2B_{66}^s)d_{112}v_0$$
$$+ B_{22}^s d_{222}v_0 - D_{11}^s d_{1111}w_b - 2(D_{12}^s + 2D_{66}^s)d_{1122}w_b$$
$$- D_{22}^s d_{2222}w_b - H_{11}^s d_{1111}w_s - 2(H_{12}^s + 2H_{66}^s)d_{1122}w_s$$
$$- H_{22}^s d_{2222}w_s + A_{55}^s d_{11}w_s + A_{44}^s d_{22}w_s = p_4 \tag{23e}$$

where $\{p\} = \{p_1, p_2, p_3, p_4\}^t$ is a generalized force vector, d_{ij}, d_{ijl} and d_{ijm} are the following differential operators

$$d_{ij} = \frac{\partial^2}{\partial x_i \partial x_j}, \quad d_{ijl} = \frac{\partial^3}{\partial x_i \partial x_j \partial x_l}, \quad d_{ijlm} = \frac{\partial^4}{\partial x_i \partial x_j \partial x_l \partial x_m}, \quad d_i = \frac{\partial}{\partial x_i}, \quad (i,j,l,m = 1,2). \tag{24}$$

The components of the generalized force vector $\{p\}$ are given by

$$p_1 = \frac{\partial N_x^T}{\partial x}, \quad p_2 = \frac{\partial N_y^T}{\partial y}, \quad p_3 = -\frac{\partial^2 M_x^{bT}}{\partial x^2} - \frac{\partial^2 M_y^{bT}}{\partial y^2}, \quad p_4 = -\frac{\partial^2 M_x^{sT}}{\partial x^2} - \frac{\partial^2 M_y^{sT}}{\partial y^2}, \tag{25}$$

3. Exact solution for a simply-supported FGM sandwich plate

Rectangular plates are generally classified in accordance with the type of support used. We are here concerned with the exact solution of Eqs. (23a)-(23e) for a simply supported FGM plate. The following boundary conditions are imposed at the side edges for RHSDT

$$v_0 = w_b = w_s = \frac{\partial w_s}{\partial y} = N_x = M_x^b = M_x^s = 0 \quad \text{at} \quad x = -a/2, \, a/2 \tag{26a}$$

$$u_0 = w_b = w_s = \frac{\partial w_s}{\partial x} = N_y = M_y^b = M_y^s = 0 \quad \text{at} \quad y = -b/2, \, b/2 \tag{26b}$$

To solve this problem, Navier presented the transverse temperature loads T_1, T_2, and T_3 in the form of a double trigonometric series as

$$\begin{Bmatrix} T_1 \\ T_2 \\ T_3 \end{Bmatrix} = \begin{Bmatrix} \overline{T}_1 \\ \overline{T}_2 \\ \overline{T}_3 \end{Bmatrix} \sin(\lambda x) \sin(\mu y) \tag{27}$$

where $\lambda = \pi / a$, $\mu = \pi / b$, $\overline{T}_1$, $\overline{T}_2$ and $\overline{T}_3$ are constants.

Following the Navier solution procedure, we assume the following solution form for u_0, v_0, w_b and w_s that satisfies the boundary conditions

$$\begin{Bmatrix} u_0 \\ v_0 \\ w_b \\ w_s \end{Bmatrix} = \begin{Bmatrix} U \cos(\lambda x)\sin(\mu y) \\ V \sin(\lambda x)\cos(\mu y) \\ W_b \sin(\lambda x)\sin(\mu y) \\ W_s \sin(\lambda x)\sin(\mu y) \end{Bmatrix}, \tag{28}$$

where U, V, W_b, and W_s are arbitrary parameters to be determined subjected to the condition that the solution in Eq. (28) satisfies governing Eq. (23). One obtains the following operator equation,

$$[K]\{\Delta\} = \{P\}, \tag{29}$$

where $\{\Delta\} = \{U, V, W_b, W_s\}^t$ and $[K]$ is the symmetric matrix given by

$$[K] = \begin{bmatrix} a_{11} & a_{12} & a_{13} & a_{14} \\ a_{12} & a_{22} & a_{23} & a_{24} \\ a_{13} & a_{23} & a_{33} & a_{34} \\ a_{14} & a_{24} & a_{34} & a_{44} \end{bmatrix}, \tag{30}$$

in which

$$\begin{aligned}
a_{11} &= -\left(A_{11}\lambda^2 + A_{66}\mu^2\right) \\
a_{12} &= -\lambda\mu\left(A_{12} + A_{66}\right) \\
a_{13} &= \lambda\left[B_{11}\lambda^2 + (B_{12} + 2B_{66})\mu^2\right] \\
a_{14} &= \lambda\left[B_{11}^s\lambda^2 + (B_{12}^s + 2B_{66}^s)\mu^2\right] \\
a_{22} &= -\left(A_{66}\lambda^2 + A_{22}\mu^2\right) \\
a_{23} &= \mu\left[(B_{12} + 2B_{66})\lambda^2 + B_{22}\mu^2\right] \\
a_{24} &= \mu\left[(B_{12}^s + 2B_{66}^s)\lambda^2 + B_{22}^s\mu^2\right] \\
a_{33} &= -\left(D_{11}\lambda^4 + 2(D_{12} + 2D_{66})\lambda^2\mu^2 + D_{22}\mu^4\right) \\
a_{34} &= -\left(D_{11}^s\lambda^4 + 2(D_{12}^s + 2D_{66}^s)\lambda^2\mu^2 + D_{22}^s\mu^4\right) \\
a_{44} &= -\left(H_{11}^s\lambda^4 + 2(H_{11}^s + 2H_{66}^s)\lambda^2\mu^2 + H_{22}^s\mu^4 + A_{55}^s\lambda^2 + A_{44}^s\mu^2\right)
\end{aligned} \tag{31}$$

The components of the generalized force vector $\{P\} = \{P_1, P_2, P_3, P_4\}^t$ are given by

$$\begin{aligned}
P_1 &= \lambda\left(A^T\overline{T}_1 + B^T\overline{T}_2 + {}^aB^T\overline{T}_3\right), \\
P_2 &= \mu\left(A^T\overline{T}_1 + B^T\overline{T}_2 + {}^aB^T\overline{T}_3\right), \\
P_3 &= -h\left(\lambda^2 + \mu^2\right)\left(B^T\overline{T}_1 + D^T\overline{T}_2 + {}^aD^T\overline{T}_3\right), \\
P_4 &= -h\left(\lambda^2 + \mu^2\right)\left({}^sB^T\overline{T}_1 + {}^sD^T\overline{T}_2 + {}^sF^T\overline{T}_3\right)
\end{aligned} \tag{32}$$

where

$$\left\{A^T, B^T, D^T\right\} = \sum_{n=1}^{3} \int_{h_{n-1}}^{h_n} \frac{E^{(n)}}{1-\left[v^{(n)}\right]^2}\left(1+v^{(n)}\right)\alpha^{(n)}\left\{1,\bar{z},\bar{z}^2\right\}dz, \tag{33a}$$

$$\left\{{}^a B^T, {}^a D^T\right\} = \sum_{n=1}^{3} \int_{h_{n-1}}^{h_n} \frac{E^{(n)}}{1-\left[v^{(n)}\right]^2}\left(1+v^{(n)}\right)\alpha^{(n)}\overline{\Psi}(z)\left\{1,\bar{z}\right\}dz, \tag{33b}$$

$$\left\{{}^s B^T, {}^s D^T, {}^s F^T\right\} = \sum_{n=1}^{3} \int_{h_{n-1}}^{h_n} \frac{E^{(n)}}{1-\left[v^{(n)}\right]^2}\left(1+v^{(n)}\right)\alpha^{(n)}\overline{f}(z)\left\{1,\bar{z},\overline{\Psi}(z)\right\}dz. \tag{33c}$$

in which $\bar{z} = z/h$, $\overline{f}(z) = f(z)/h$ and $\overline{\Psi}(z) = \Psi(z)/h$.

For further computational reasons the converted expressions of the stress components are also recorded. They read

$$\sigma_{xx}^{(n)} = \frac{E^{(n)}}{1-\left[v^{(n)}\right]^2}\left\{-\left(\lambda U + v^{(n)}\mu V\right) - z\left(\lambda^2 + v\mu^2\right)W_b - f(z)\left(\lambda^2 + v\mu^2\right)W_s\right.$$
$$\left. -\left(1+v\right)\alpha^{(n)}\left(\overline{T}_1 + \bar{z}\overline{T}_2 + \overline{T}_3\overline{\Psi(z)}\right)\right\}\sin(\lambda x)\sin(\mu y), \tag{34a}$$

$$\sigma_{yy}^{(n)} = \frac{E^{(n)}}{1-\left[v^{(n)}\right]^2}\left\{-\left(v^{(n)}\lambda U + \mu V\right) - z\left(v\lambda^2 + \mu^2\right)W_b - f(z)\left(v\lambda^2 + \mu^2\right)W_s\right.$$
$$\left. -\left(1+v\right)\alpha^{(n)}\left(\overline{T}_1 + \bar{z}\overline{T}_2 + \overline{T}_3\overline{\Psi(z)}\right)\right\}\sin(\lambda x)\sin(\mu y), \tag{34b}$$

$$\tau_{xy}^{(n)} = \frac{E^{(n)}}{2(1+v^{(n)})}\left\{U\mu + \lambda V - 2zW_b\lambda\mu - 2f(z)W_s\lambda\mu\right\}\cos(\lambda x)\cos(\mu y) \tag{34c}$$

$$\tau_{yz}^{(n)} = \frac{E^{(n)}}{2(1+v^{(n)})}g(z)W_s\mu\sin(\lambda x)\cos(\mu y) \tag{34d}$$

$$\tau_{xz}^{(n)} = \frac{E^{(n)}}{2(1+v^{(n)})}g(z)W_s\lambda\cos(\lambda x)\sin(\mu y). \tag{34e}$$

4. Numerical results and discussion

The thermoelastic bending analysis is conducted for combinations of metal and ceramic. The set of materials chosen is Titanium and Zirconia. For simplicity, Poisson's ratio of the two materials is assigned the same value. Typical values for metal and ceramics used in the FG sandwich plate are listed in Table 1.

To illustrate the preceding thermal–structural analysis, a variety of sample problems is considered. For the sake of brevity, only linearly varying (across the thickness) temperature distribution $T = \bar{z}T_2$; non-linearly varying (across the thickness) temperature distribution $T = \overline{\Psi}(z)T_3$; and a combination of both $T = \bar{z}T_2 + \overline{\Psi}(z)T_3$ are considered. Note that, in most of

Table 1 Material properties used in the FG sandwich plate

Properties	Metal: Ti–6A1–4V	Ceramic: ZrO_2
E (GPa)	66.2	117.0
v	1/3	1/3
α (10^{-6}/K)	10.3	7.11

Table 2 Dimensionless center deflections $\overline{w}$ of the different sandwich square plates ($\overline{T}_3 = 0$)

k	Theory	$\overline{w}$				
		1-0-1	1-1-1	1-2-1	2-1-2	2-2-1
0	RHSDT	0.4802624102	0.4802624102	0.4802624102	0.4802624102	0.4802624102
	PSDPT	0.4802624102	0.4802624102	0.4802624102	0.4802624102	0.4802624102
	SSDPT	0.4802624102	0.4802624102	0.4802624102	0.4802624102	0.4802624102
	ESDPT	0.4802624103	0.4802624103	0.4802624103	0.4802624103	0.4802624103
	FSDPT	0.4802624102	0.4802624102	0.4802624102	0.4802624102	0.4802624102
1	RHSDT	0.6368706308	0.6062263692	0.5822683070	0.6210413648	0.5925388921
	PSDPT	0.6368913262	0.6062561495	0.5823018576	0.6210669479	0.5925682404
	SSDPT	0.6369163694	0.6062923043	0.5823425647	0.6210979535	0.5926037400
	ESDPT	0.6369414052	0.6063285913	0.5823832496	0.6211290262	0.5926390742
	FSDPT	0.6366671314	0.6059360027	0.5819321936	0.6207916196	0.5922391382
2	RHSDT	0.6714713237	0.6392955205	0.6097919038	0.6560934439	0.6215132668
	PSDPT	0.6714858174	0.6393248874	0.6098293922	0.6561154815	0.6215438592
	SSDPT	0.6715034090	0.6393606439	0.6098750470	0.6561422528	0.6215809264
	ESDPT	0.6715211425	0.6393968398	0.6099210670	0.6561692997	0.6216180116
	FSDPT	0.6713392117	0.6390276350	0.6094377060	0.6558929929	0.6212148977
3	RHSDT	0.6835507403	0.6536111265	0.6223824709	0.6702345950	0.6341090637
	PSDPT	0.6835604161	0.6536381567	0.6224203294	0.6702526802	0.6341386760
	SSDPT	0.6835722007	0.6536711126	0.6224665084	0.6702746869	0.6341745670
	ESDPT	0.6835841674	0.6537046290	0.6225132536	0.6702970392	0.6342105448
	FSDPT	0.6834673554	0.6533737951	0.6220352754	0.6700774890	0.6338263885
4	RHSDT	0.6887884431	0.6612355282	0.6294497079	0.6772877664	0.6408768475
	PSDPT	0.6887950624	0.6612604942	0.6294872146	0.6773029321	0.6409054051
	SSDPT	0.6888031547	0.6612909572	0.6295330002	0.6773214139	0.6409400177
	ESDPT	0.6888114260	0.6613220299	0.6295794618	0.6773402624	0.6409747420
	FSDPT	0.6887337861	0.6610216386	0.6291117804	0.6771602164	0.6406073812
5	RHSDT	0.6914100554	0.6658457922	0.6339205284	0.6813141649	0.6450084220
	PSDPT	0.6914147346	0.6658691382	0.6339575524	0.6813272417	0.6450361194
	SSDPT	0.6914204743	0.6658976406	0.6340027691	0.6813431982	0.6450696862
	ESDPT	0.6914263743	0.6659267720	0.6340487255	0.6813595221	0.6451033721
	FSDPT	0.6913726822	0.6656490845	0.6335907572	0.6812067429	0.6447488688

A. Bouchafa, M.B. Bouiadjra, M.S.A. Houari and A. Tounsi
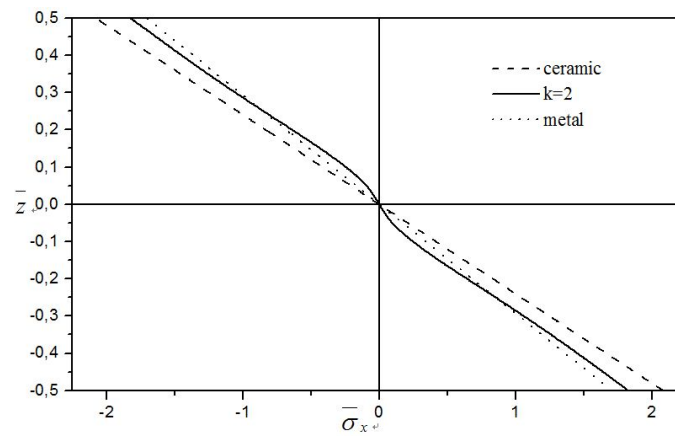

(a)
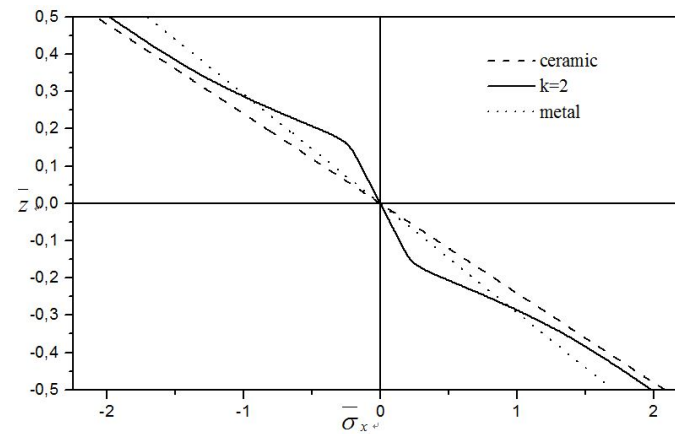
(b)
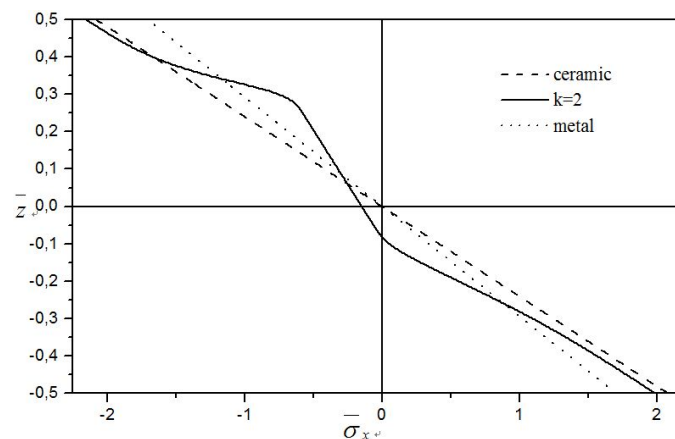
(c)

Fig. 3 Variation of axial stress $\overline{\sigma}_x$ through the plate thickness for different types of sandwich plates: (a) The (1-0-1) FGM sandwich plate; (b) the (1-1-1) FGM sandwich plate; and (c) the (2-2-1) FGM sandwich plate

the literature, the thermal stress problems are treated under a steady state temperature distribution that is linear with respect to the thickness direction.

Different dimensionless quantities are used for pure temperature loading as:

- center deflection $\overline{w} = \dfrac{h}{\alpha_0 \overline{\overline{T}}_2 \, a^2} \, w\left(\dfrac{a}{2}, \dfrac{b}{2}\right)$,

- axial stress $\overline{\sigma}_x = \dfrac{h^2}{\alpha_0 \overline{\overline{T}}_2 \, E_0 \, a^2} \, \sigma_x\left(\dfrac{a}{2}, \dfrac{b}{2}, \dfrac{h}{2}\right)$,

- shear stress $\overline{\tau}_{xz} = \dfrac{10h}{\alpha_0 \overline{\overline{T}}_2 \, E_0 \, a} \, \tau_{xz}\left(0, \dfrac{b}{2}, 0\right)$.

where the reference values are taken as $E_0 = 1$ GPa and $\alpha_0 = 10^{-6}/$K. Numerical results are presented in Tables 2-5 using different plate theories. Additional results are plotted in Figs. 2-5 using the present refined hyperbolic shear deformation theory (RHSDT). It is assumed, unless otherwise stated, that $a / h = 10$, $a / b = 1$, $\overline{T}_1 = 0$ and $\overline{T}_2 = 100$: The shear correction factor of FSDPT is fixed to be K = 5/6.

Table 2 contains the dimensionless center deflection $\overline{w}$ for an FG sandwich plate subjected to thermal field varying linearly through the thickness $(\overline{T}_3 = 0)$. The deflections are considered for k = 0, 1, 2, 3, 4, and 5 and different types of sandwich plates. Table 2 shows that the effect of shear deformation is to increase the deflection. The difference between the shear deformation theories is insignificant for fully ceramic plates ($k = 0$). It can be observed that the results obtained by the present refined hyperbolic shear deformation theory (RHSDT) are identical to those of the parabolic shear deformation plate theory (PSDPT).

Table 3 compares the deflections of different types of the FGM rectangular sandwich plates with $k = 3$. The deflections decrease as the aspect ratio a / b increases and this irrespective of the type of the sandwich plate.

Table 4 lists values of axial stress $\overline{\sigma}_x$ for $k = 0$, 1, 2, 3, 4, and 5 and different types of sandwich plates. Once again, the plate is subjected to a thermal field varying linearly through its thickness. All theories (Present, PSDPT, SSDPT, ESDPT and FSDPT) give the same axial stress $\overline{\sigma}_x$ for a fully ceramic plate ($k = 0$). In general, the axial stress decreases (in absolute value) as k increases.

Table 5 shows similar results of transverse shear stress $\overline{\tau}_{xz}$ for FGM sandwich plate subjected to a combination of linearly and non-linearly thermal field $(\overline{T}_3 = -100)$. The relative difference between RHSDT (present refined hyperbolic shear deformation theory) and the other shear deformation theories may be stable for different values of k and this irrespective of the type of the FGM sandwich plate.

It is to be noted that the CPT yields identical center deflections and axial stresses with the FSDPT and so Tables 2-4 lack the results of CPT. In addition, the transverse shear stresses as per the FSDPT are indistinguishable and so Table 5 lacks the results of FSDPT. It can be observed that the results obtained by the present refined hyperbolic shear deformation theory (RHSDT) are identical to those of the parabolic shear deformation plate theory (PSDPT). In general, the fully ceramic plates give the smallest deflections, transverse shear stresses. As the volume fraction exponent increases for FG plates, the deflection and axial stress will increase. In fact the non-symmetric (2-2-1) FGM plate yields the smallest axial stresses. But the symmetric (2-1-2) FGM plate yields the smallest transverse shear stresses.

Table 3 Effect of aspect ratio a/b on the dimensionless deflection of the FGM sandwich plates ($k = 3$, $\overline{T}_3 = 0$)

Scheme	Theory	$\overline{w}$				
		$a/b=1$	$a/b=2$	$a/b=3$	$a/b=4$	$a/b=5$
1-0-1	RHSDT	0.6835507403	0.2734702662	0.1367766934	0.08049100480	0.05265731134
	PSDPT	0.6835604161	0.2734799211	0.1367863142	0.08050057789	0.05266682333
	SSDPT	0.6835722007	0.2734916748	0.1367980164	0.08051220862	0.05267836270
	ESDPT	0.6835841674	0.2735036028	0.1368098802	0.08052398306	0.05269002373
	FSDPT	0.6834673554	0.2733869420	0.1366934709	0.08040792405	0.05257441194
1-1-1	RHSDT	0.6536111265	0.2615866858	0.1309116553	0.07710402281	0.05049555491
	PSDPT	0.6536381567	0.2616136607	0.1309385381	0.07713077677	0.05052214456
	SSDPT	0.6536711126	0.2616465325	0.1309712706	0.07716331532	0.05055443573
	ESDPT	0.6537046290	0.2616799433	0.1310045062	0.07719630764	0.05058711818
	FSDPT	0.6533737951	0.2613495179	0.1306747589	0.07686750522	0.05025952271
1-2-1	RHSDT	0.6223824709	0.2491610666	0.1247536140	0.07352662427	0.04819415962
	PSDPT	0.6224203294	0.2491988441	0.1247912569	0.07356407967	0.04823137579
	SSDPT	0.6224665084	0.2492449004	0.1248371096	0.07360964929	0.04827658433
	ESDPT	0.6225132536	0.2492914914	0.1248834449	0.07365562907	0.04832211149
	FSDPT	0.6220352754	0.2488141101	0.1244070550	0.07318062062	0.04784886733
2-1-2	RHSDT	0.6702345950	0.2681879937	0.1341723150	0.07898921053	0.05170066414
	PSDPT	0.6702526802	0.2682060416	0.1341903021	0.07900711268	0.05171845750
	SSDPT	0.6702746869	0.2682279928	0.1342121614	0.07902884445	0.05174002622
	ESDPT	0.6702970392	0.2682502760	0.1342343297	0.07905085315	0.05176183188
	FSDPT	0.6700774890	0.2680309957	0.1340154977	0.07883264575	0.05154442227
2-2-1	RHSDT	0.6341090637	0.2538130370	0.1270474362	0.07484951752	0.04903700521
	PSDPT	0.6341386760	0.2538425841	0.1270768764	0.07487880905	0.04906610667
	SSDPT	0.6341745670	0.2538783787	0.1271125106	0.07491422011	0.04910123314
	ESDPT	0.6342105448	0.2539142358	0.1271481680	0.07494960009	0.04913625980
	FSDPT	0.6338263885	0.2535305552	0.1267652777	0.07456781021	0.04875587597

Table 4 Dimensionless axial stresses $\overline{\sigma}_x$ of the FGM sandwich square plates ($\overline{T}_3 = 0$)

k	Theory	$\overline{\sigma}_x$				
		1-0-1	1-1-1	1-2-1	2-1-2	2-2-1
0	RHSDT	-2.079675000	-2.079675000	-2.079675000	-2.079675000	-2.079675000
	PSDPT	-2.079675000	-2.079675000	-2.079675000	-2.079675000	-2.079675000
	SSDPT	-2.079675000	-2.079675000	-2.079675000	-2.079675000	-2.079675000
	ESDPT	-2.079675000	-2.079675000	-2.079675000	-2.079675000	-2.079675000
	FSDPT	-2.079675000	-2.079675000	-2.079675000	-2.079675000	-2.079675000

Table 4 Continued

k	Theory	$\overline{\sigma}_x$				
		1-0-1	1-1-1	1-2-1	2-1-2	2-2-1
	RHSDT	-1.993949024	-2.144463137	-2.262047306	-2.071702695	-2.276249844
	PSDPT	-1.993921201	-2.144422272	-2.262000494	-2.071667914	-2.276208646
1	SSDPT	-1.993884786	-2.144368665	-2.261939156	-2.071622328	-2.276154795
	ESDPT	-1.993845490	-2.144310614	-2.261873016	-2.071573038	-2.276096911
	FSDPT	-1.994116421	-2.144706898	-2.262331770	-2.071910534	-2.276503415
	RHSDT	-1.824107609	-1.982324788	-2.127244698	-1.899739614	-2.152914653
	PSDPT	-1.824088994	-1.982285282	-2.127192581	-1.899710605	-2.152871650
2	SSDPT	-1.824064523	-1.982233209	-2.127123963	-1.899672432	-2.152815257
	ESDPT	-1.824037920	-1.982176362	-2.127049363	-1.899630827	-2.152754300
	FSDPT	-1.824214263	-1.982549342	-2.127547647	-1.899904728	-2.153169938
	RHSDT	-1.764716957	-1.912052225	-2.065519569	-1.830269330	-2.099337320
	PSDPT	-1.764704974	-1.912016606	-2.065467370	-1.830246217	-2.099295847
3	SSDPT	-1.764689178	-1.911969550	-2.065398481	-1.830215732	-2.099241393
	ESDPT	-1.764671900	-1.911917944	-2.065323270	-1.830182347	-2.099182378
	FSDPT	-1.764783222	-1.912249450	-2.065816299	-1.830397030	-2.099579373
	RHSDT	-1.738933325	-1.874596642	-2.030851542	-1.795587171	-2.070463527
	PSDPT	-1.738925338	-1.874564258	-2.030800203	-1.795568206	-2.070423669
4	SSDPT	-1.738914769	-1.874521431	-2.030732364	-1.795543156	-2.070371300
	ESDPT	-1.738903150	-1.874474330	-2.030658117	-1.795515624	-2.070314469
	FSDPT	-1.738976349	-1.874773038	-2.031139594	-1.795689836	-2.070694054
	RHSDT	-1.726015831	-1.851936073	-2.008911087	-1.775774941	-2.052760285
	PSDPT	-1.726010283	-1.851906151	-2.008860704	-1.775758844	-2.052721725
5	SSDPT	-1.726002920	-1.851866541	-2.008794079	-1.775737554	-2.052671042
	ESDPT	-1.725994791	-1.851822901	-2.008721038	-1.775714098	-2.052616010
	FSDPT	-1.726045075	-1.852097357	-2.009191452	-1.775860809	-2.052982076

Table 5 Dimensionless axial stresses $\overline{\tau}_{xz}$ of the FGM sandwich square plates $(\overline{T}_3 = -100)$

k	Theory	$\overline{\tau}_{xz}$				
		1-0-1	1-1-1	1-2-1	2-1-2	2-2-1
	RHSDT	0.3875715824	0.3875715824	0.3875715824	0.3875715824	0.3875715824
	PSDPT	0.4663492274	0.4663492274	0.4663492274	0.4663492274	0.4663492274
0	SSDPT	0.5740631176	0.5740631176	0.5740631176	0.5740631176	0.5740631176
	ESDPT	0.6962208109	0.6962208324	0.6962208104	0.6962208280	0.6962208236
	RHSDT	0.4670021493	0.4617811853	0.4664858752	0.4600158773	0.4634957554
1	PSDPT	0.5640586115	0.5599566926	0.5669251263	0.5566617108	0.5622309572

Table 5 Continued

k	Theory	$\bar{\tau}_{xz}$				
		1-0-1	1-1-1	1-2-1	2-1-2	2-2-1
1	SSDPT	0.6967738614	0.6948170803	0.7052694992	0.6890771075	0.6979014024
	ESDPT	0.8478429561	0.8493472298	0.8642891414	0.8402733375	0.8533361303
2	RHSDT	0.4702713211	0.4598648679	0.4701346983	0.4563344392	0.4653381807
	PSDPT	0.5658813664	0.5567693568	0.5715458768	0.5505668090	0.5640619895
	SSDPT	0.6960436985	0.6896201730	0.7112661898	0.6791942164	0.6995711498
	ESDPT	0.8433472288	0.8415995173	0.8720815362	0.8254402890	0.8547138864
3	RHSDT	0.4737529709	0.4560245642	0.4701572347	0.4520107054	0.4645262663
	PSDPT	0.5687108270	0.5512369044	0.5713193563	0.5440270977	0.5625135986
	SSDPT	0.6976345415	0.6815157927	0.7106268240	0.6692561998	0.6968497094
	ESDPT	0.8429437758	0.8302322625	0.8709425017	0.8110896408	0.8504454017
4	RHSDT	0.4784793386	0.4526303727	0.4693704507	0.4489858559	0.4635472624
	PSDPT	0.5736245062	0.5464635339	0.5701170738	0.5394455140	0.5608927464
	SSDPT	0.7026165109	0.6746640867	0.7087816096	0.6622911958	0.6942257194
	ESDPT	0.8476509530	0.8207453411	0.8682981840	0.8010142924	0.8465038762
5	RHSDT	0.4837367333	0.4499549506	0.4684276059	0.4471214799	0.4627809680
	PSDPT	0.5795305375	0.5427240764	0.5687710112	0.5365261496	0.5596420018
	SSDPT	0.7093154867	0.6693258637	0.7068213417	0.6577478799	0.6922203248
	ESDPT	0.8550478520	0.8133777300	0.8655727331	0.7943293272	0.8435042530

Fig 3 contains the plots of the axial stress $\bar{\sigma}_x$ through-the-thickness of the FGM sandwich plates. The stresses are tensile below the mid-plane and compressive above the mid-plane except for the nonsymmetric (2-2-1) FGM plate. The axial stress is continuous through the plate thickness. The results demonstrate a nonlinear variation of the axial stress through the plate thickness for $k = 2$. All types of FGM plate yield the maximum compressive (minimum tensile) stress at the top (bottom) surface of the core layer. These are the ceramic-rich surfaces in which the ceramic plate experiences the minimum compressive or maximum tensile stresses.

In Fig. 4 we have plotted the through-the-thickness distributions of the transverse shear stress $\bar{\tau}_{xz}$: The maximum value occurs at a point on the mid-plane of the plate and its magnitude for FGM plate is between that for homogeneous plates (ceramic and metal plates) except for the (1-0-1) FGM plate.

In Figs. 5 and 6 we have plotted the through-the-thickness distributions of the dimensionless axial stress $\bar{\sigma}_x$ and the transverse shear stress $\bar{\tau}_{xz}$ through-the-thickness of the (1-1-1) FGM plate ($k = 2$). These results reveal that the variation of stresses is very sensitive to the variation of the thermal load $\bar{T}_3$ value.

In Figs. 5 and 6 we have plotted the through-the-thickness distributions of the dimensionless axial stress $\bar{\sigma}_x$ and the transverse shear stress $\bar{\tau}_{xz}$ through-the-thickness of the (1-2-1) FGM plate ($k = 1.5$). These results reveal that the variation of stresses is very sensitive to the variation of the thermal load $\bar{T}_3$ value.
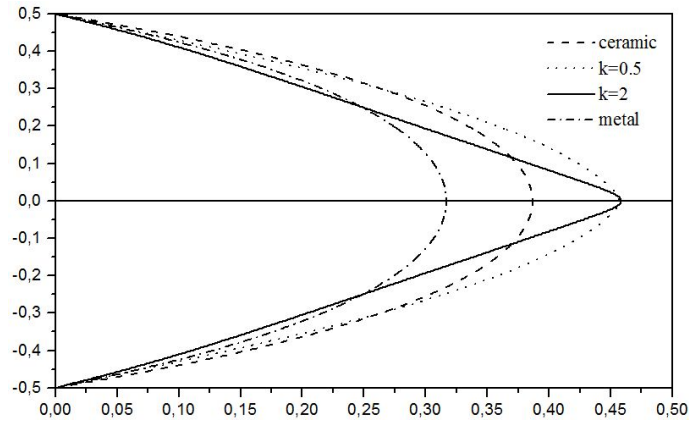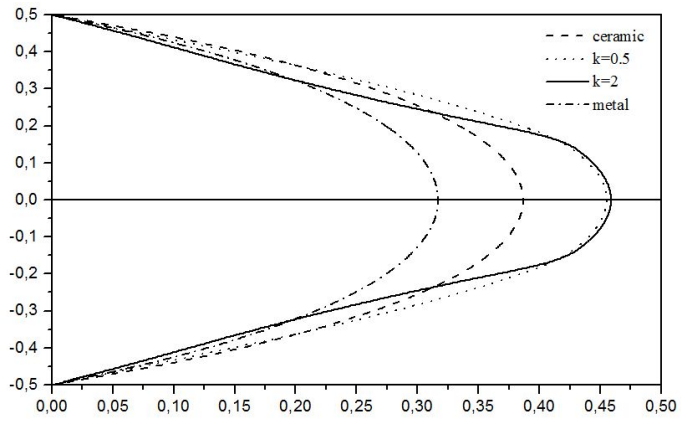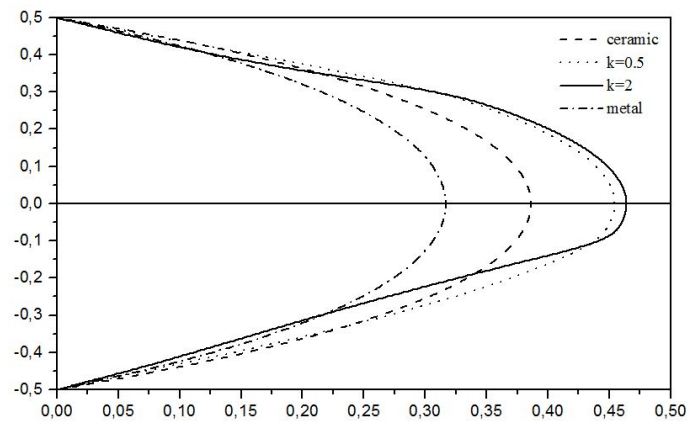
Fig. 4 Variation of transverse shear stress $\bar{\tau}_{xz}$ through the plate thickness for different types of sandwich plates: (a) The (1-0-1) FGM sandwich plate; (b) the (1-1-1) FGM sandwich plate; and (c) the (2-2-1) FGM sandwich plate
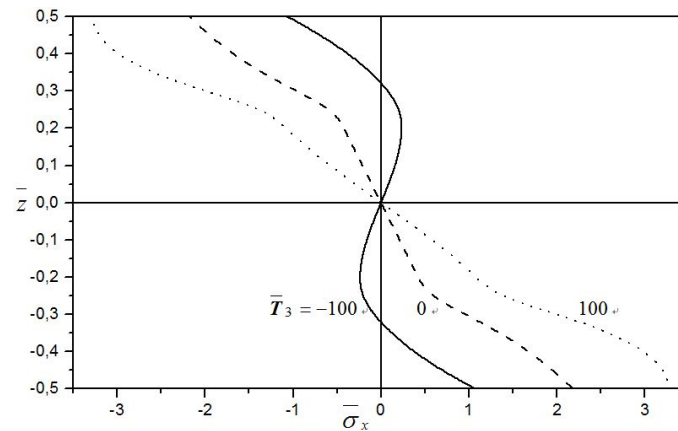
Fig. 5 Effect of the thermal load $\overline{T}_3$ on the axial stress $\overline{\sigma}_x$ of the (1-2-1) FGM sandwich plate ($k = 1.5$)
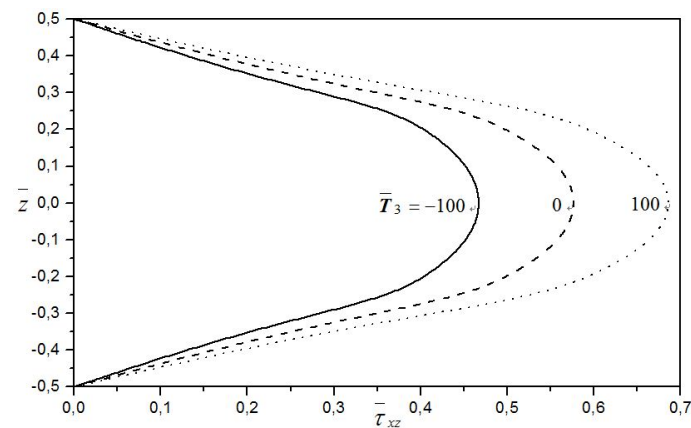

Fig. 6 Effect of the thermal load $\overline{T}_3$ on the transverse shear stress $\overline{\tau}_{xz}$ of the (1-2-1) FGM sandwich plate ($k = 1.5$)

5. Conclusions

The thermoelastic bending response of FGM sandwich plates is studied using a new refined hyperbolic shear deformation theory (RHSDT). The number of primary variables in this theory is even less than that of first- and higher-order shear deformation plate theories. The theory gives parabolic distribution of transverse shear strains, and satisfies the zero traction boundary conditions on the surfaces of the plate without using shear correction factors. All comparison studies demonstrated that the deflections and the thermal stresses obtained using the present refined theory (with four unknowns) and other higher order shear deformation theories (five unknowns) are almost identical. Hence, it can be said that the proposed theory RHSDT is accurate and simple in solving the thermoelastic bending behavior of FG plates. The formulation lends itself particularly well to finite element simulations (Curiel Sosa *et al*. 2012, 2013) and also other numerical methods employing symbolic computation for plate bending problems (Rashidi *et al*. 2012), which will be considered in the near future.

References

Ait Amar Meziane, M., Abdelaziz, H.H. and Tounsi, A. (2014), "An efficient and simple refined theory for buckling and free vibration of exponentially graded sandwich plates under various boundary conditions", *J. Sandw. Struct. Mater.*, **16**(3), 293-318.

Ait Yahia, S., Ait Atmane, H., Houari, M.S.A. and Tounsi, A. (2015), "Wave propagation in functionally graded plates with porosities using various higher-order shear deformation plate theories", *Struct. Eng. Mech.*, *Int. J.*, **53**(6), 1143-1165.

Attia, A., Tounsi, A., Adda Bedia, E.A. and Mahmoud, S.R. (2015), "Free vibration analysis of functionally graded plates with temperature-dependent properties using various four variable refined plate theories", *Steel Compos. Struct.*, *Int. J.*, **18**(1), 187-212.

Bachir Bouiadjra, R., Adda Bedia, E.A. and Tounsi, A. (2013), "Nonlinear thermal buckling behavior of functionally graded plates using an efficient sinusoidal shear deformation theory", *Struct. Eng. Mech.*, *Int. J.*, **48**(4), 547-567.

Belabed, Z., Houari, M.S.A., Tounsi, A., Mahmoud, S.R. and Anwar Bég, O. (2014), "An efficient and simple higher order shear and normal deformation theory for functionally graded material (FGM) plates", *Compos.: Part B*, **60**, 274-283.

Benachour, A., Daouadji, H.T., Ait Atmane, H., Tounsi, A. and Meftah, S.A. (2011), "A four variable refined plate theory for free vibrations of functionally graded plates with arbitrary gradient", *Compos. Part B*, **42**(6), 1386-1394.

Bessaim, A., Houari, M.S.A., Tounsi, A., Mahmoud, S.R. and Adda Bedia, E.A. (2013), "A new higher-order shear and normal deformation theory for the static and free vibration analysis of sandwich plates with functionally graded isotropic face sheets", *J. Sandw. Struct. Mater.*, **15**(6), 671-703.

Bouderba, B., Houari, M.S.A. and Tounsi, A. (2013) "Thermomechanical bending response of FGM thick plates resting on Winkler–Pasternak elastic foundations", *Steel Compos. Struct.*, *Int. J.*, **14**(1), 85-104.

Bourada, M., Tounsi, A., Houari, M.S.A. and Adda Bedia, E.A. (2012), "A new four-variable refined plate theory for thermal buckling analysis of functionally graded sandwich plates", *J. Sandw. Struct. Mater.*, **14**(1), 5-33.

Bourada, M., Kaci, A., Houari, M.S.A. and Tounsi, A. (2015), "A new simple shear and normal deformations theory for functionally graded beams", *Steel Compos. Struct.*, *Int. J.*, **18**(2), 409-423.

Bousahla, A.A., Houari, M.S.A., Tounsi, A. and Adda Bedia, E.A. (2014), "A novel higher order shear and normal deformation theory based on neutral surface position for bending analysis of advanced composite plates", *Int. J. Comput. Method.*, **11**(6), 1350082.

Chakraverty, S. and Pradhan, K.K. (2014), "Free vibration of exponential functionally graded rectangular plates in thermal environment with general boundary conditions", *Aerosp. Sci. Technol.*, **36**, 132-156.

Curiel Sosa, J.L., Munoz, J.J., Pinho, S.T. and Anwar Bég, O. (2012), "(XFEM) Simulation of damage in laminates", *Proceedings of Applied Sciences and Engineering* (*ECCOMAS 2012*), (J. Eberhardsteiner *et al.* Eds.), Vienna, Austria, September.

Curiel Sosa, J.L., Anwar Bég, O. and Liebana Murillo, J.M. (2013), "Finite element analysis of structural instability using a switching implicit-explicit technique", *Int. J. Comp. Method. Eng. Sci. Mech.*, **14**(5), 452-464.

Delale, F. and Erdogan, F. (1983), "The crack problem for a nonhomogeneous plane", *J. Appl. Mech.*, **50**(3), 609-707.

Draiche, K., Tounsi, A. and Khalfi, Y. (2014), "A trigonometric four variable plate theory for free vibration of rectangular composite plates with patch mass", *Steel Compos. Struct.*, *Int. J.*, **17**(1), 69-81.

El Meiche, N., Tounsi, A., Ziane, N., Mechab, I. and Adda Bedia, E.A. (2011), "A new hyperbolic shear deformation theory for buckling and vibration of functionally graded sandwich plate", *Int. J. Mech. Sci.*, **53**(4), 237-247.

Fekrar, A., Houari, M.S.A., Tounsi, A. and Mahmoud, S.R. (2014), "A new five-unknown refined theory based on neutral surface position for bending analysis of exponential graded plates", *Meccanica*, **49**(4),

795-810.

Finot, M. and Suresh, S. (1996), "Small and large deformation of thick and thin-film multi-layers: effect of layer geometry, plasticity and compositional gradients", *J. Mech. Phys. Solid.*, **44**(5), 683-721.

Hamidi, A., Houari, M.S.A., Mahmoud, S.R. and Tounsi, A. (2015), "A sinusoidal plate theory with 5-unknowns and stretching effect for thermomechanical bending of functionally graded sandwich plates", *Steel Compos. Struct., Int. J.*, **18**(1), 235-253.

Hebali, H., Tounsi, A., Houari, M.S.A., Bessaim, A. and Adda Bedia, E.A. (2014), "New quasi-3D hyperbolic shear deformation theory for the static and free vibration analysis of functionally graded plates", *J. Eng. Mech.* (*ASCE*), **140**(2), 374-383.

Houari, M.S.A., Tounsi, A. and Anwar Bég, O. (2013), "Thermoelastic bending analysis of functionally graded sandwich plates using a new higher order shear and normal deformation theory", *Int. J. Mech. Sci.*, **76**, 102-111.

Jha, D.K., Kant, T. and Singh, R.K. (2013), "A critical review of recent research on functionally graded plates", *Compos. Struct.*, **96**, 833-849.

Karama, M., Afaq, K.S. and Mistou, S. (2003), "Mechanical behaviour of laminated composite beam by the new multi-layered laminated composite structures model with transverse shear stress continuity", *Int. J. Solids Struct.*, **40**(6), 1525-1546.

Khalfi, Y., Houari, M.S.A. and Tounsi, A. (2014), "A refined and simple shear deformation theory for thermal buckling of solar functionally graded plates on elastic foundation", *Int. J. Comput. Method.*, **11**(5), 135007.

Lu, C.F., Lim, C.W. and Chen, W.Q. (2009), "Semi-analytical analysis for multi-directional functionally graded 509 plates: 3-d elasticity solutions", *Int. J. Numer. Meth. Eng.*, **79**(1), 25-44.

Mahi, A., Adda Bedia, E.A. and Tounsi, A. (2015), "A new hyperbolic shear deformation theory for bending and free vibration analysis of isotropic, functionally graded, sandwich and laminated composite plates", *Appl. Math. Model.*, **39**(9), 2489-2508.

Mantari, J.L. and Granados, E.V. (2015), "Thermoelastic analysis of advanced sandwich plates based on a new quasi-3D hybrid type HSDT with 5 unknowns", *Compos.: Part B*, **69**, 317-334.

Marur, P.R. (1999), "Fracture behaviour of functionally graded materials", Ph.D. Thesis; Auburn University, AL, USA.

Nedri, K., El Meiche, N. and Tounsi, A. (2014), "Free vibration analysis of laminated composite plates resting on elastic foundations by using a refined hyperbolic shear deformation theory", *Mech. Compos. Mater.*, **49**(6), 641-650.

Obata, Y. and Noda, N. (1994), "Steady thermal stresses in a hollow circular cylinder and a hollow sphere of a functionally gradient material", *J. Ther. Stresses*, **17**(3), 471-488.

Ould Larbi, L., Kaci, A., Houari, M.S.A. and Tounsi, A. (2013), "An efficient shear deformation beam theory based on neutral surface position for bending and free vibration of functionally graded beams", *Mech. Based Des. Struct. Mach.*, **41**(4), 421-433.

Praveen, G.N., Chin, C.D. and Reddy, J.N. (1999), "Thermoelastic analysis of functionally graded ceramic-metal cylinder", *J. Eng. Mech.*, **125**(11), 1259-1267.

Rashidi, M.M., Shooshtari, A. and Anwar Bég, O. (2012), "Homotopy perturbation study of nonlinear vibration of Von Kármán rectangular plates", *Comput. Struct.*, **106/107**, 46-55.

Reddy, J.N. (1984), "A simple higher-order theory for laminated composite plates", *J. Appl. Mech.*, **51**(4), 745–752.

Reddy, J.N. and Chin, C.D. (1998), "Thermoelastic analysis of functionally graded cylinders and plates", *J. Ther. Stresses*, **21**(6), 593-626.

Swaminathan, K. and Naveenkumar, D.T. (2014), "Higher order refined computational models for the stability analysis of FGM plates – Analytical solutions", *European J. Mech. A/Solids*, **47**, 349-361.

Talha, M. and Singh, B.N. (2010), "Static response and free vibration analysis of FGM plates using higher order shear deformation theory", *Appl. Math. Model*, **34**(12), 3991-4011.

Tounsi, A., Houari, M.S.A., Benyoucef, S. and Adda Bedia, E.A. (2013), "A refined trigonometric shear deformation theory for thermoelastic bending of functionally graded sandwich plates", *Aerosp. Sci.*

Techol., **24**(1), 209-220.

Touratier, M. (1991), "An efficient standard plate theory", *Int. J. Eng. Sci.*, **29**(0), 901-916.

Vel, S.S. and Batra, R.C. (2002), "Exact thermoelasticity solution for functionally graded thick rectangular plates", *AIAA J.*, **40**(7), 1421-1433.

Vel, S.S. and Batra, R.C. (2003), "Three-dimensional analysis of transient thermal stresses in functionally graded plates", *Int. J. Solids Struct.*, **40**(25), 7181-7196.

Wen, P.H., Sladek, J. and Sladek, V. (2011), "Three-dimensional analysis of functionally graded plates", *Int. J. Numer. Meth. Eng.*, **87**(10), 923-942.

Yaghoobi, H. and Fereidoon, A. (2014), "Mechanical and thermal buckling analysis of functionally graded plates resting on elastic foundations: An assessment of a simple refined nth-order shear deformation theory", *Compos.: Part B*, **62**, 54-64.

Yaghoobi, H. and Torabi, M. (2013a), "Post-buckling and nonlinear free vibration analysis of geometrically imperfect functionally graded beams resting on nonlinear elastic foundation", *Appl. Math. Model.*, **37**(18-19), 8324-8340.

Yaghoobi, H. and Torabi, M. (2013b), "Exact solution for thermal buckling of functionally graded plates resting on elastic foundations with various boundary conditions", *J. Therm. Stress.*, **36**(9), 869-894.

Yaghoobi, H. and Yaghoobi, P. (2013), "Buckling analysis of sandwich plates with FGM face sheets resting on elastic foundation with various boundary conditions: An analytical approach", *Meccanica*, **48**(8), 2019-2035.

Ying, J., Lü, C.F. and Lim, C.W. (2009), "3D thermoelasticity solutions for functionally graded thick plates", *J. Zhejiang Univ. Sci A*, **10**(3), 327-336.

Zidi, M., Tounsi, A., Houari, M.S.A., Adda Bedia, E.A. and Anwar Bég, O. (2014), "Bending analysis of FGM plates under hygro-thermo-mechanical loading using a four variable refined plate theory", *Aerosp. Sci. Technol.*, **34**, 24-34.

CC